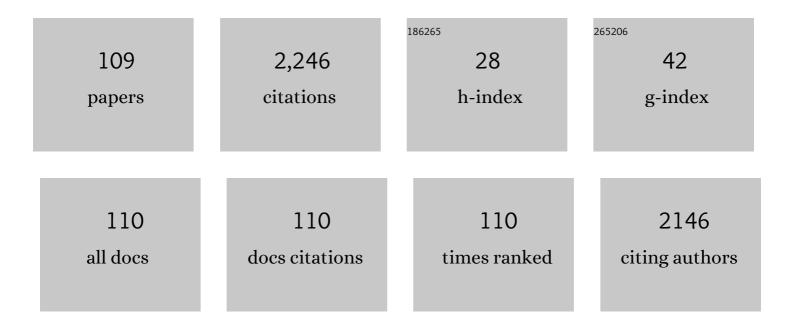
## Arvo Kikas

## List of Publications by Year in descending order

Source: https://exaly.com/author-pdf/1154850/publications.pdf Version: 2024-02-01



ADVO KIKAS

#	Article	IF	CITATIONS
1	Mesoporous textured Fe-N-C electrocatalysts as highly efficient cathodes for proton exchange membrane fuel cells. Journal of Power Sources, 2022, 520, 230819.	7.8	46
2	Liquid-assisted grinding/compression: a facile mechanosynthetic route for the production of high-performing Co–N–C electrocatalyst materials. Green Chemistry, 2022, 24, 305-314.	9.0	8
3	Transition metal and nitrogen-doped mesoporous carbons as cathode catalysts for anion-exchange membrane fuel cells. Applied Catalysis B: Environmental, 2022, 306, 121113.	20.2	42
4	Nitrogen and Phosphorus Dual-Doped Silicon Carbide-Derived Carbon/Carbon Nanotube Composite for the Anion-Exchange Membrane Fuel Cell Cathode. ACS Applied Energy Materials, 2022, 5, 2949-2958.	5.1	21
5	Polypyrrole and Polythiophene Modified Carbon Nanotubeâ€Based Cathode Catalysts for Anion Exchange Membrane Fuel Cell. ChemElectroChem, 2022, 9, .	3.4	9
6	Cobalt-Containing Nitrogen-Doped Carbon Materials Derived from Saccharides as Efficient Electrocatalysts for Oxygen Reduction Reaction. Catalysts, 2022, 12, 568.	3.5	3
7	Characterisation of Novel Nitrogen Doped Reduced Graphene Oxide. ECS Transactions, 2022, 108, 99-109.	0.5	0
8	Electroreduction of oxygen on cobalt phthalocyanine-modified carbide-derived carbon/carbon nanotube composite catalysts. Journal of Solid State Electrochemistry, 2021, 25, 57-71.	2.5	37
9	Transition metal-containing nitrogen-doped nanocarbon catalysts derived from 5-methylresorcinol for anion exchange membrane fuel cell application. Journal of Colloid and Interface Science, 2021, 584, 263-274.	9.4	50
10	Transition metal phthalocyanine-modified shungite-based cathode catalysts for alkaline membrane fuel cell. International Journal of Hydrogen Energy, 2021, 46, 4365-4377.	7.1	36
11	Non-precious metal cathodes for anion exchange membrane fuel cells from ball-milled iron and nitrogen doped carbide-derived carbons. Renewable Energy, 2021, 167, 800-810.	8.9	50
12	Transition-Metal- and Nitrogen-Doped Carbide-Derived Carbon/Carbon Nanotube Composites as Cathode Catalysts for Anion-Exchange Membrane Fuel Cells. ACS Catalysis, 2021, 11, 1920-1931.	11.2	85
13	Multi-purpose heterogeneous catalyst material from an amorphous cobalt metal–organic framework. Materials Advances, 2021, 2, 4009-4015.	5.4	6
14	Bifunctional multi-metallic nitrogen-doped nanocarbon catalysts derived from 5-methylresorcinol. Electrochemistry Communications, 2021, 124, 106932.	4.7	16
15	Silicon carbide-derived carbon electrocatalysts dual doped with nitrogen and phosphorus for the oxygen reduction reaction in an alkaline medium. Electrochemistry Communications, 2021, 125, 106976.	4.7	24
16	Mesoporous iron-nitrogen co-doped carbon material as cathode catalyst for the anion exchange membrane fuel cell. Journal of Power Sources Advances, 2021, 8, 100052.	5.1	43
17	Synthesis and Characterization of Cobalt and Nitrogen Co-Doped Peat-Derived Carbon Catalysts for Oxygen Reduction in Acidic Media. Catalysts, 2021, 11, 715.	3.5	6
18	Bimetal Phthalocyanineâ€Modified Carbon Nanotubeâ€Based Bifunctional Catalysts for Zincâ€Air Batteries. ChemElectroChem, 2021, 8, 2662-2670.	3.4	34

#	Article	IF	CITATIONS
19	Atomic-layer design and properties of Pr-doped HfO2 thin films. Journal of Alloys and Compounds, 2021, 868, 159100.	5.5	4
20	Bifunctional Oxygen Electrocatalysis on Mixed Metal Phthalocyanine-Modified Carbon Nanotubes Prepared via Pyrolysis. ACS Applied Materials & Interfaces, 2021, 13, 41507-41516.	8.0	65
21	Iron and cobalt containing electrospun carbon nanofibre-based cathode catalysts for anion exchange membrane fuel cell. International Journal of Hydrogen Energy, 2021, 46, 31275-31287.	7.1	30
22	Oxygen reduction reaction on Pd nanoparticles supported on novel mesoporous carbon materials. Electrochimica Acta, 2021, 394, 139132.	5.2	14
23	Oxygen reduction reaction on Pd nanocatalysts prepared by plasma-assisted synthesis on different carbon nanomaterials. Nanotechnology, 2021, 32, 035401.	2.6	8
24	Multivariable oxygen sensing based on photoluminescence and photoconductivity of TiO2 nanoparticles. Sensors and Actuators B: Chemical, 2020, 303, 127236.	7.8	6
25	Electrocatalytic oxygen reduction reaction on iron phthalocyanine-modified carbide-derived carbon/carbon nanotube composite electrocatalysts. Electrochimica Acta, 2020, 334, 135575.	5.2	50
26	Impact of ball-milling of carbide-derived carbons on the generation of hydrogen peroxide via electroreduction of oxygen in alkaline media. Journal of Electroanalytical Chemistry, 2020, 878, 114690.	3.8	19
27	Electrospun Polyacrylonitrileâ€Derived Co or Fe Containing Nanofibre Catalysts for Oxygen Reduction Reaction at the Alkaline Membrane Fuel Cell Cathode. ChemCatChem, 2020, 12, 4568-4581.	3.7	31
28	Effects of N and O groups for oxygen reduction reaction on one- and two-dimensional carbonaceous materials. Electrochimica Acta, 2020, 344, 136052.	5.2	23
29	Peat-derived carbon-based non-platinum group metal type catalyst for oxygen reduction and evolution reactions. Electrochemistry Communications, 2020, 113, 106700.	4.7	12
30	Nitrogen-doped carbide-derived carbon/carbon nanotube composites as cathode catalysts for anion exchange membrane fuel cell application. Applied Catalysis B: Environmental, 2020, 272, 119012.	20.2	72
31	Cobalt and Nitrogen Co-Doped Peat Derived Carbon Based Catalysts for Oxygen Reduction. ECS Transactions, 2020, 97, 605-613.	0.5	1
32	Platinum Sputtered on Nb-doped TiO <sub>2</sub> Films Prepared by ALD: Highly Active and Durable Carbon-free ORR Electrocatalyst. Journal of the Electrochemical Society, 2020, 167, 164505.	2.9	13
33	Transition Metal-Containing Nitrogen-Doped Nanocarbons Derived from 5-Methylresorcinol for Anion Exchange Membrane Fuel Cell Application. ECS Meeting Abstracts, 2020, MA2020-02, 2361-2361.	0.0	0
34	The electronic structure of ionic liquids based on the TFSI anion: A gas phase UPS and DFT study. Journal of Molecular Liquids, 2019, 294, 111580.	4.9	10
35	Sulphur and nitrogen co-doped graphene-based electrocatalysts for oxygen reduction reaction in alkaline medium. Electrochemistry Communications, 2019, 109, 106603.	4.7	46
36	Effect of Ball-Milling on the Oxygen Reduction Reaction Activity of Iron and Nitrogen Co-doped Carbide-Derived Carbon Catalysts in Acid Media. ACS Applied Energy Materials, 2019, 2, 7952-7962.	5.1	36

#	Article	IF	CITATIONS
37	UPS and DFT investigation of the electronic structure of gas-phase trimesic acid. Journal of Electron Spectroscopy and Related Phenomena, 2016, 213, 11-16.	1.7	4
38	Study of the structural phase transformation of iron oxide nanoparticles from an Fe2+ ion source by precipitation under various synthesis parameters and temperatures. Materials Chemistry and Physics, 2015, 149-150, 473-479.	4.0	37
39	The benefit of the European User Community from transnational access to national radiation facilities. Journal of Synchrotron Radiation, 2014, 21, 638-639.	2.4	2
40	In Situ XPS Studies of Electrochemically Negatively Polarized Molybdenum Carbide Derived Carbon Double Layer Capacitor Electrode. Journal of the Electrochemical Society, 2013, 160, A1084-A1093.	2.9	25
41	Electronic structure of LBO and BBO as revealed by boron and oxygen RIXS spectra. Journal of Electron Spectroscopy and Related Phenomena, 2013, 188, 32-37.	1.7	1
42	Structural and Magnetic Studies on Iron Oxide and Iron-Magnesium Oxide Thin Films Deposited Using Ferrocene and (Dimethylaminomethyl)ferrocene Precursors. ECS Journal of Solid State Science and Technology, 2013, 2, N45-N54.	1.8	23
43	Effect of different annealing temperatures and SiO <sub>2</sub> /Si(100) substrate on the properties of nickel containing titania thin sol–gel films. Physica Status Solidi (A) Applications and Materials Science, 2012, 209, 953-965.	1.8	10
44	Vacuum ultraviolet and X-ray emission spectroscopy of anion and cation excitons in oxide crystals. Journal of Surface Investigation, 2012, 6, 100-105.	0.5	1
45	The sub-bandgap energy loss satellites in the RIXS spectra of beryllium compounds. Journal of Electron Spectroscopy and Related Phenomena, 2011, 184, 366-370.	1.7	2
46	Effect of cobalt doping and annealing on properties of titania thin films prepared by sol–gel process. Applied Surface Science, 2011, 257, 6897-6907.	6.1	31
47	Physical and electrochemical characteristics of supercapacitors based on carbide derived carbon electrodes in aqueous electrolytes. Journal of Power Sources, 2011, 196, 4109-4116.	7.8	94
48	Combined luminescence and X-ray emission study of self-trapped excitons in oxides. IOP Conference Series: Materials Science and Engineering, 2010, 15, 012088.	0.6	2
49	Electron spectroscopic study of passive oxide layer formation on Fe–19Cr–18Ni–1Al–TiC austenitic stainless steel. Journal of Electron Spectroscopy and Related Phenomena, 2010, 182, 108-114.	1.7	6
50	Influence of the heating temperature on the properties of nickel doped TiO2 films prepared by sol–gel method. Applied Surface Science, 2010, 256, 4538-4542.	6.1	12
51	Resonant inelastic x-ray scattering and UV–VUV luminescence at the Be 1s edge in BeO. Journal of Physics Condensed Matter, 2010, 22, 375505.	1.8	2
52	Pt coated Cr2O3 thin films for resistive gas sensors. Open Physics, 2009, 7, .	1.7	3
53	Surface analysis of spray deposited copper indium disulfide films. Thin Solid Films, 2008, 516, 7110-7115.	1.8	42
54	Substrate-induced effects in the creation and decay of potassium 2p core excitations in ultrathin films of KCl on copper. Journal of Physics Condensed Matter, 2008, 20, 145206.	1.8	6

#	Article	IF	CITATIONS
55	Effect of phase composition on X-ray absorption spectra of ZrO2 thin films. Journal of Electron Spectroscopy and Related Phenomena, 2007, 156-158, 303-306.	1.7	13
56	Substrate-induced effects in the creation and decay of core excitations in ultrathin films of potassium chloride on copper. Journal of Electron Spectroscopy and Related Phenomena, 2007, 156-158, 294-298.	1.7	0
57	Resonant inelastic X-ray scattering at the Be 1s edge in BeO. Journal of Electron Spectroscopy and Related Phenomena, 2007, 156-158, 299-302.	1.7	6
58	XPS and AFM investigation of hafnium dioxide thin films prepared by atomic layer deposition on silicon. Journal of Electron Spectroscopy and Related Phenomena, 2007, 156-158, 150-154.	1.7	16
59	Inner-shell excitation of intrinsic luminescence and resonantly excited X-ray fluorescence at Be 1s edge in oriented BeO crystals. Nuclear Instruments and Methods in Physics Research, Section A: Accelerators, Spectrometers, Detectors and Associated Equipment, 2007, 575, 172-175.	1.6	4
60	Resonant inelastic X-ray scattering at the K edge of oxygen and fluorine in insulators. Journal of Electron Spectroscopy and Related Phenomena, 2005, 144-147, 845-848.	1.7	3
61	Engineering structure and properties of hafnium oxide films by atomic layer deposition temperature. Thin Solid Films, 2005, 479, 1-11.	1.8	36
62	Insulating properties of ultrathin KF layers on Cu(100): Resonant Auger spectroscopy. Surface Science, 2005, 584, 49-54.	1.9	8
63	Resonant inelastic x-ray scattering at the F1sphotoabsorption edge in LiF: Interplay of excitonic and conduction states, and Stokes' doubling. Physical Review B, 2004, 70, .	3.2	10
64	Potential barrier effects in Cs 3d resonance photoemission of CsF. Journal of Electron Spectroscopy and Related Phenomena, 2004, 137-140, 377-381.	1.7	3
65	Effects of precursors on nucleation in atomic layer deposition of HfO2. Applied Surface Science, 2004, 230, 292-300.	6.1	39
66	Limitations of the ionic model in describing core-hole decayÂmolecular versus crystalline KCl. Journal of Physics B: Atomic, Molecular and Optical Physics, 2003, 36, L85-L91.	1.5	15
67	Na K PHOTOABSORPTION AND RESONANT KLL AUGER SPECTRA IN NaF AND NaCl. Surface Review and Letters, 2002, 09, 1303-1308.	1.1	3
68	Study of Thin Oxide Films by Electron, Ion and Synchrotron Radiation Beams. Mikrochimica Acta, 2002, 139, 165-169.	5.0	13
69	Core excitons in NaKphotoabsorption of NaF: Resonant Auger spectroscopy. Physical Review B, 2001, 64, .	3.2	13
70	Multi-atom resonant photoemission in transition metal chlorides. Solid State Communications, 2000, 115, 275-279.	1.9	20
71	Vibrationally selective resonant Auger spectroscopy in CO: evidence of the valence character of the 3s `Rydberg level'. Journal of Physics B: Atomic, Molecular and Optical Physics, 1999, 32, 267-275.	1.5	6
72	Resonant photoemission of CoCl2. Journal of Electron Spectroscopy and Related Phenomena, 1999, 101-103, 745-749.	1.7	6

#	Article	IF	CITATIONS
73	Resonant auger spectra of TiO2 at Ti2p and O1s absorption edges. Journal of Electron Spectroscopy and Related Phenomena, 1998, 93, 193-199.	1.7	14
74	Angle-resolved spectator decay of vibrationally selected C 1s(2σ)â~12Ï€1 excited states in carbon monoxide. Journal of Electron Spectroscopy and Related Phenomena, 1998, 95, 25-36.	1.7	12
75	Continuum resonance in ethylene: Evidence from vibrationally resolved core photoionization. Physical Review A, 1998, 58, 1879-1884.	2.5	28
76	Influences from the C1sshape resonance on the vibrational progression in the Auger decay of CO. Physical Review A, 1998, 58, 2037-2042.	2.5	19
77	Auger decay of core-excited higher Rydberg states of carbon monoxide. Journal of Physics B: Atomic, Molecular and Optical Physics, 1997, 30, 4267-4278.	1.5	14
78	Vibrationally selective resonant Auger spectroscopy of the3pcore-to-Rydberg excitation in CO. Physical Review A, 1997, 56, 480-487.	2.5	17
79	The vibrationally resolved C 1s core photoelectron spectra of methane and ethane. Journal of Chemical Physics, 1997, 106, 1661-1668.	3.0	69
80	Collapse of Vibrational Structure in the Auger Resonant Raman Spectrum of CO by Frequency Detuning. Physical Review Letters, 1997, 79, 1451-1454.	7.8	85
81	Ti 2p and O 1s X-ray absorption of TiO2 polymorphs. Solid State Communications, 1997, 104, 199-203.	1.9	105
82	High-resolution study of the correlation satellites in photoelectron spectra of the rare gases. Journal of Electron Spectroscopy and Related Phenomena, 1996, 77, 241-266.	1.7	116
83	Siteâ€selective participator decay of coreâ€excited butadiene. Journal of Chemical Physics, 1996, 105, 10719-10724.	3.0	15
84	Interplay of atomic and solid-state effects in inner-shell-resonant photoelectron spectra. Physical Review B, 1996, 53, R5978-R5981.	3.2	7
85	Auger decay of the dissociating coreâ€excited states in the HCl and DCl molecules. Journal of Chemical Physics, 1996, 104, 4475-4480.	3.0	51
86	Auger and photoelectron spectra of K+ in solids at resonant 2p6 to 2p53d excitation. Journal of Electron Spectroscopy and Related Phenomena, 1995, 72, 127-131.	1.7	5
87	L23MM resonnant auger spectra of Mn in KMnF3. Journal of Electron Spectroscopy and Related Phenomena, 1995, 72, 113-117.	1.7	1
88	MNN resonant Auger spectra of Ce in CeCl3. Journal of Electron Spectroscopy and Related Phenomena, 1995, 72, 119-123.	1.7	3
89	3d-Resonant photo- and auger emission of Ce in CeO2. Journal of Electron Spectroscopy and Related Phenomena, 1995, 76, 583-587.	1.7	1
90	Appearance of crystal-field splitting in 2p-resonant electron spectra of K+ in ionic solids. Journal of Electron Spectroscopy and Related Phenomena, 1995, 76, 589-594.	1.7	3

#	Article	IF	CITATIONS
91	NEXAFS of ionic solids as seen through resonant electron spectra. Physica B: Condensed Matter, 1995, 208-209, 47-48.	2.7	1
92	2p-3dresonant Auger scattering byK+ions ofKMnF3without the influence of the crystal-field splitting. Physical Review B, 1995, 51, 3202-3205.	3.2	6
93	High-resolution photoelectron satellite spectrum of He excited by synchrotron radiation at 96.5 eV photon energy. Journal of Physics B: Atomic, Molecular and Optical Physics, 1995, 28, L293-L297.	1.5	17
94	K+LMMresonant Auger spectra of solid KF. Physical Review B, 1994, 50, 9079-9085.	3.2	10
95	M4,5N4,5N4,5Auger decay spectra of the resonantly excited 3d94fconfiguration of xenonlike ions in solids. Physical Review B, 1994, 49, 14836-14844.	3.2	7
96	Character of F core excitons in alkali fluorides studied by resonant Auger spectroscopy. Physical Review B, 1994, 49, 3116-3123.	3.2	22
97	Auger decay processes of resonantly excited 3dâ^'14f configuration of xenon-like ions in solids. Journal of Electron Spectroscopy and Related Phenomena, 1994, 68, 277-286.	1.7	5
98	Autoionization phenomena involving the 2p53d configuration of argon-like ions in ionic solids. Journal of Electron Spectroscopy and Related Phenomena, 1994, 68, 287-296.	1.7	8
99	Autoionization phenomena involving the 2p53dconfiguration of argonlike ions in ionic solids. Physical Review B, 1993, 47, 11736-11748.	3.2	61
100	Auger Decay of K+L23Excitations in Potassium Halides. Physica Scripta, 1992, T41, 237-240.	2.5	5
101	Probing of electron-phonon scattering in ionic solids by XUV-induced electron emission spectroscopy. Surface Science, 1992, 269-270, 583-589.	1.9	2
102	Auger Transitions as Luminescence Killers in Ionic Solids. Physica Scripta, 1992, T41, 19-22.	2.5	1
103	Monte Carlo simulation of the cross-luminescence excitation spectrum in a CsBr crystal. Nuclear Instruments and Methods in Physics Research, Section A: Accelerators, Spectrometers, Detectors and Associated Equipment, 1991, 308, 211-214.	1.6	2
104	Auger Spectra of K <sup>+</sup> <i>L</i> <sub>23</sub> Excitations in Potassium Halides. Europhysics Letters, 1991, 15, 683-686.	2.0	9
105	Secondary photoelectron spectra of NaCl and KBr excited by XUV radiation: Experiments and computer simulations. Solid State Communications, 1990, 76, 1383-1386.	1.9	4
106	Monte Carlo simulation of the crossluminescence excitation spectrum in a CSBR crystal. Solid State Communications, 1990, 76, 1313-1316.	1.9	10
107	Monte Carlo Simulation of Electron–Phonon Scattering in the XUVâ€Induced Electron Emission of NaCl. Physica Status Solidi (B): Basic Research, 1986, 137, 495-500.	1.5	15
108	Monte Carlo Simulation of the Production of Charge Carriers in NaCl Crystals by XUV Irradiation. Physica Status Solidi (B): Basic Research, 1985, 130, 211-218.	1.5	14

#	Article	IF	CITATIONS
109	The quantum yield spectra of electron emission of solids in XUV region. Physica Status Solidi (B): Basic Research, 1982, 114, 487-493.	1.5	9